

## RESEARCH ARTICLE

[View Article Online](#)  
[View Journal](#) | [View Issue](#)

 Cite this: *Mater. Chem. Front.*,  
 2018, 2, 2286

# Cholesterol-based diazine derivative: selective sensing of Ag<sup>+</sup> and Fe<sup>3+</sup> ions through gelation and the performance of metallogels in dye and picric acid adsorption from water†

Atanu Panja and Kumares Ghosh  \*

Cholesterol appended diazine derivative **1** on a 4-hydroxybenzaldehyde scaffold has been designed and synthesized. The compound having diazine as a metal ion binding site forms nice gels with Ag<sup>+</sup> and Fe<sup>3+</sup> ions over a series of other metal ions from CHCl<sub>3</sub>/CH<sub>3</sub>OH (3:1, v/v). Strong hydrophobic interaction owing to the presence of cholesterol has a marked contribution in aggregation. The SEM image reveals fibrillar to globular porous microstructures. The true nature of the gels is determined from a rheological study. The Ag<sup>+</sup> and Fe<sup>3+</sup>-gels are distinguishable with the aid of tetrabutylammonium chloride, tetrabutylammonium bromide or fluoride and ammonium thiocyanate. There is no interference of Fe<sup>2+</sup> ions in the detection of Fe<sup>3+</sup> ions. The presence of Fe<sup>2+</sup> ions in solution can successfully be ascertained through gelation of **1** in the specified solvent upon adding external oxidising agents such as *m*-CPBA. As an application, both the Ag<sup>+</sup>- and Fe<sup>3+</sup>-gels of **1** act as good adsorbents for adsorption of uranine dye and picric acid from aqueous solution. In this process, the metallogels are recyclable and exhibit excellent efficiency.

 Received 28th August 2018,  
 Accepted 4th October 2018

DOI: 10.1039/c8qm00433a

rsc.li/frontiers-materials

## Introduction

Selective sensing and visualization of biologically significant analytes through prolific use of low molecular weight supramolecular gelators (LMWGs) have become an ongoing research interest in recent times.<sup>1</sup> Low molecular weight supramolecular gelators (LMWGs) under weak noncovalent forces establish a cross-linked network in solution due to which gel formation occurs.<sup>2</sup> The self-organization of such gelator molecules can be tuned by regulating the weak forces using external physical or chemical stimuli (light, redox, pH, ions).<sup>3</sup> Chemical stimuli-induced changes in gel properties are beneficial for the development of new molecular sensors.<sup>1–3</sup>

In continuation of our ongoing research interest in developing stimuli responsive supramolecular gelators on a 4-hydroxybenzaldehyde-cholesterol platform,<sup>4</sup> we herein wish to report a simple, easy to make diazine functionalized LMWG **1** which performs excellently in metal ion sensing with practical applications. The hydrazine-based dipodal symmetrical imines

(1,4-disubstituted azines or diazines) are well known metal chelators and they are successfully used in various colorimetric and fluorescent sensors.<sup>5</sup> This class of ligands possess delocalized electron density on the C=N–N=C bond. Binding of metal ions to the diazine motif restricts the free rotation of the N–N bond and displays optical feedback. Compounds with this functionality are also known to exhibit interesting properties like excited state intramolecular proton transfer (ESIPT), aggregation induced emission enhancement (AIEE) *etc.*<sup>5g</sup> Considering all these properties, the designed compound **1** was selected which formed nice gels from a CHCl<sub>3</sub>/CH<sub>3</sub>OH mixture solvent in the presence of Ag<sup>+</sup> and Fe<sup>3+</sup> ions. The metallogels have applications in various aspects. Here, they are established to be useful in discrimination of halides, dye adsorption and picric acid removal from waste water.

Fig. 1 represents the different components of gelator **1**. While the cholesterol motif has been introduced for assisting self-aggregation of the molecules through hydrophobic interaction,<sup>6</sup> the diazine bridge is used as the site of metal ion interaction with an expectation of influencing the gelation property of compound **1** (either gel-to-sol or *vice versa*). Moreover, the use of a large hydrophobic surface in the design has a discernible impact on dye adsorption in the aggregated state.<sup>1g,4c</sup>

Among the different analytes, sensing and detection of Ag<sup>+</sup> and Fe<sup>3+</sup> ions draw much attention because of their biological significance.<sup>7</sup> Although, Ag<sup>+</sup> ions have broad applications in

Department of Chemistry, University of Kalyani, Kalyani-741235, India.

E-mail: ghosh\_k2003@yahoo.co.in, kumareschem18@klyuniv.ac.in;

Fax: +91-3325828282; Tel: +91-3325828750 ext. 305

 † Electronic supplementary information (ESI) available: Figures showing the gelation profile, gel pics, FTIR data, UV-vis titration plots of **1** with various metal ions, binding constant and detection limit plots and other spectral plots, comparison table, and characterization spectra. See DOI: 10.1039/c8qm00433a

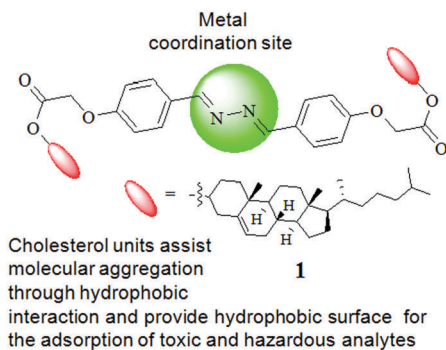


Fig. 1 Design concept and structure of compound **1**.

organic synthesis, electronics, photography, mirrors and pharmacy, the release of a large quantity of silver to the environment causes toxic contamination which becomes a threat to aquatic and living organisms.<sup>8</sup> On the other hand,  $\text{Fe}^{3+}$  ions are an essential element in living cells playing crucial roles in the function of haemoglobin.<sup>9</sup> Their deficiency can damage several body functions and lead to liver damage, anaemia, Alzheimer's and Parkinson's diseases *etc.*<sup>9</sup> Therefore, an approach for the easy and efficient detection of  $\text{Ag}^+$  and  $\text{Fe}^{3+}$  ions, especially in sol-gel medium, is worth investigating. Although there are plenty number of reports on their fluorometric detection,<sup>10</sup> the detection of  $\text{Fe}^{3+}$  and  $\text{Ag}^+$  using LMWGs and their subsequent applications in material chemistry is less explored.<sup>4b,11,12</sup>

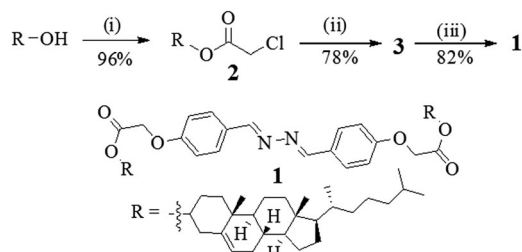
## Results and discussion

### Synthesis

Compound **1** was synthesized according to Scheme 1. Initially, cholesterol was converted to the chloro ester **2** which upon reflux with 4-hydroxy benzaldehyde in the presence of  $\text{K}_2\text{CO}_3$  in  $\text{CH}_3\text{CN}$  gave the cholesteryl aldehyde **3**.<sup>4</sup> Schiff base formation between the aldehyde **3** and hydrazine in dry benzene afforded the corresponding diazine derivative **1** in appreciable yield. All the compounds were fully characterized by usual spectroscopic methods.

### Gelation and metal responsive character

The gel forming ability of compound **1** was investigated in different solvents (Table S1, ESI<sup>†</sup>). Compound **1** remained



**Scheme 1** (i) Chloroacetyl chloride, pyridine, dry  $\text{CHCl}_3$ , rt, 10 h; (ii) 4-hydroxybenzaldehyde,  $\text{K}_2\text{CO}_3$ ,  $\text{CH}_3\text{CN}$ , 5 h; (iii)  $\text{N}_2\text{H}_4 \cdot \text{H}_2\text{O}$ , dry benzene, reflux, 3 days.

practically insoluble in most of the semi-aqueous solvents (except in  $\text{THF-H}_2\text{O}$ , where it gave solution). It was partially soluble in polar solvents like DMF, DMSO or  $\text{CH}_3\text{CN}$ . Interestingly, in toluene, it underwent aggregation to form a gel. However, the toluene gel was unstable and broken down on slight disturbance. This was a hindrance to investigating the metal ion sensitivity of **1** by sol-gel methodology.

Therefore, the influence of different metal ions in bringing gelation of **1** in different solvent compositions was verified. It was found that in  $\text{THF/H}_2\text{O}$  (1 : 1, v/v), metal ions like  $\text{Cu}^{2+}$ ,  $\text{Ag}^+$  and  $\text{Hg}^{2+}$  ions gave precipitation, whereas in  $\text{CHCl}_3/\text{CH}_3\text{OH}$  (3 : 1, v/v) compound **1** readily formed stable gels in the presence of  $\text{Ag}^+$  and  $\text{Fe}^{3+}$  ions (Table S1, ESI<sup>†</sup>). So, for detailed investigation, the  $\text{CHCl}_3/\text{CH}_3\text{OH}$  (3 : 1, v/v) solvent combination was used as the desired solvent in the study.

The effect of different metal ions on gelation of **1** was investigated by adding equiv. amounts of different metal solutions (as perchlorate salts,  $c = 0.1 \text{ M}$  in  $\text{CH}_3\text{OH}$ ) to the  $\text{CHCl}_3$  solution of **1**. The volume was adjusted with the required solvent to maintain  $\text{CHCl}_3/\text{CH}_3\text{OH}$  as 3 : 1 (v/v). In this study, while  $\text{Ag}^+$  and  $\text{Fe}^{3+}$  ions resulted in gelation of **1**, other metal ions under identical conditions remained silent (Fig. 2A). Importantly, gelation also occurred upon direct addition of perchlorate salts of  $\text{Ag}^+$  and  $\text{Fe}^{3+}$  ions to the  $\text{CHCl}_3/\text{CH}_3\text{OH}$  (3 : 1, v/v) solution of **1** followed by gentle shaking. While the  $\text{Ag}^+$ -induced gel was pale yellow colored, it was orange in the case of the  $\text{Fe}^{3+}$ -induced gel. These findings suggested the high sensitivity of gelator **1** toward  $\text{Ag}^+$  and  $\text{Fe}^{3+}$  ions, rather than any other metal ions tested. Compound **1** was also able to form a stable gel under identical conditions, in the presence of other  $\text{Ag}^+$  and  $\text{Fe}^{3+}$ -salts such as  $\text{AgNO}_3$  and  $\text{Fe}(\text{NO}_3)_3$  (Fig. 2B) and thereby we neglected any role of anions of the metal salts.

### Discrimination between $\text{Ag}^+$ - and $\text{Fe}^{3+}$ -gels

Discrimination of the two metallo gels was achieved upon treatment with tetrabutylammonium chloride (TBACl) and  $\text{NH}_4\text{SCN}$  (Fig. 3). Addition of TBACl to the  $\text{Ag}^+$ -gel of **1** ruptured the gel completely, while under identical conditions, the  $\text{Fe}^{3+}$ -induced gel remained unperturbed. Upon addition of  $\text{Cl}^-$  ions, scavenging of  $\text{Ag}^+$  ions from the gel matrix took place

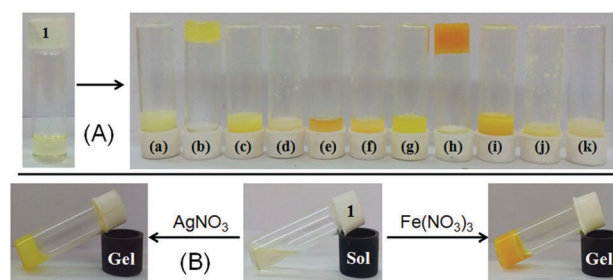


**Fig. 2** (A) Photograph showing the phase changes of **1** ( $c = 25 \text{ mg mL}^{-1}$ ) in  $\text{CHCl}_3/\text{CH}_3\text{OH}$  (3 : 1, v/v) upon addition of an equiv. amount of different metal ions (as perchlorate salts,  $c = 0.1 \text{ M}$  in  $\text{CH}_3\text{OH}$ ) after 2 h [from left to right: (a)  $\text{Cu}^{2+}$ , (b)  $\text{Ag}^+$ , (c)  $\text{Hg}^{2+}$ , (d)  $\text{Pb}^{2+}$ , (e)  $\text{Zn}^{2+}$ , (f)  $\text{Cd}^{2+}$ , (g)  $\text{Al}^{3+}$ , (h)  $\text{Fe}^{3+}$ , (i)  $\text{Fe}^{2+}$ , (j)  $\text{Ni}^{2+}$  and (k)  $\text{Co}^{2+}$ ] and (B) photograph showing the preparation of gels from **1** in the presence of  $\text{AgNO}_3$  and  $\text{Fe}(\text{NO}_3)_3$ .

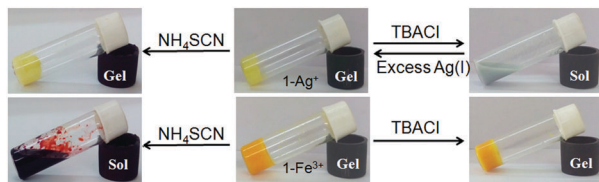


Fig. 3 Chemical responsiveness of the  $\text{Ag}^+$ -induced (top) and  $\text{Fe}^{3+}$ -induced (bottom) gels of **1** in the presence of TBACl and  $\text{NH}_4\text{SCN}$ .

for which  $\text{Ag}^+$ -induced organisation of gelator **1** was destroyed and the gel was collapsed to the sol. However, addition of excess  $\text{Ag}^+$  ions to the  $\text{Cl}^-$ -induced broken gel could again reinforce gelation. Similarly, addition of  $\text{NH}_4\text{SCN}$  to the  $1\text{-Fe}^{3+}$  gel resulted in the formation of a blood-red colored solution. In contrast, the  $1\text{-Ag}^+$  gel remained intact even after 1 h, under similar conditions. These findings corroborated the visual discrimination of the  $\text{Ag}^+$ -gel from the  $\text{Fe}^{3+}$ -gel.

### Thermal stability and morphological study of the metallogels

Prior to study, the minimum gelation concentrations (mgc) of **1** for the metal ions (counter anions: perchlorate ions) were determined. The 'mgc' values for the  $\text{Ag}^+$ - and  $\text{Fe}^{3+}$ -gels were  $16 \text{ mg mL}^{-1}$  and  $19 \text{ mg mL}^{-1}$ , respectively. Both metallogels at their respective mgc values exhibited almost a similar thermal stability ( $T_{\text{gel}} = 40\text{--}42^\circ\text{C}$ ). However, at a common concentration ( $19 \text{ mg mL}^{-1}$ ), the  $\text{Ag}^+$ -induced gel exhibited a higher gel melting temperature ( $T_{\text{gel}} = 46^\circ\text{C}$ ) than the  $\text{Fe}^{3+}$ -induced gel ( $T_{\text{gel}} = 42^\circ\text{C}$ ), indicating strong aggregation in the presence of  $\text{Ag}^+$  ions. It is mentionable that use of nitrate salts of silver and iron under identical conditions showed almost similar thermal stability (for  $\text{AgNO}_3$ :  $T_{\text{gel}} = 48^\circ\text{C}$ ; for  $\text{Fe}(\text{NO}_3)_3$ :  $T_{\text{gel}} = 40^\circ\text{C}$ ). Both the gels were thermoreversible as confirmed by the usual heating-cooling method (Fig. 4a).

To get an insight into the morphology of the metallogels, SEM images were captured. While there was an interlinked porous fibrillar network for the  $\text{Fe}^{3+}$ -metallogel (Fig. 4b and b'), a globular microstructure was observed for the  $\text{Ag}^+$ -metallogel (Fig. 4c and c').

### Probable mode of interaction during metallogelation

As the imine bonds in many cases are hydrolysed to aldehyde in the presence of metal ions,<sup>13</sup> it was necessary to check whether the gelation of **1** occurred through the formation of aldehyde **3** in the present case. For this, in the experiment it was observed that aldehyde **3** did not form a gel either in  $\text{CHCl}_3/\text{CH}_3\text{OH}$  (3 : 1, v/v) or in the presence of  $\text{Ag}^+$  and  $\text{Fe}^{3+}$  ions (Fig. S1, ESI†). NMR study as described later reveals the stability of **1**.

To understand the molecular aggregation, UV-vis and fluorescence spectra of compound **1** were compared in the sol and gel states (Fig. S2, ESI†). In solution, compound **1** exhibited an absorption band at 326 nm which was red shifted to 376 nm for the  $\text{Ag}$ -gel. Such red shift of the absorption band to 334 nm along with a weak shouldering in the region of 426 nm was observed for the  $\text{Fe}$ -gel, and corroborated the aggregation. In fluorescence, gelation caused a significant decrease in the fluorescence intensity of **1** for both the

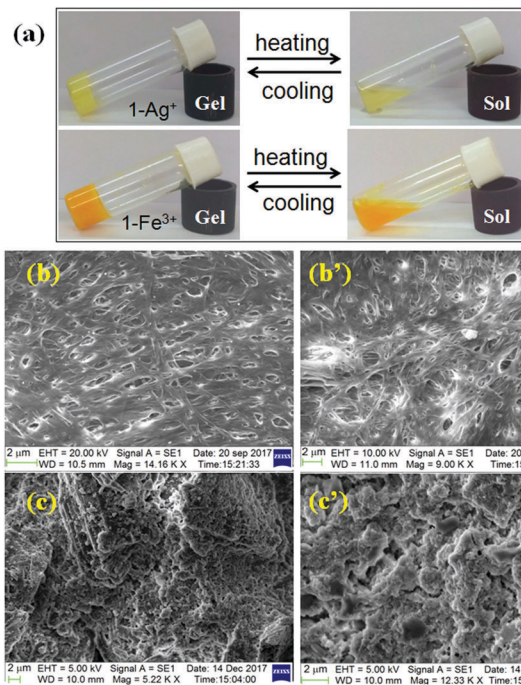


Fig. 4 (a) Photograph showing the thermo reversibility of  $\text{Ag}^+$ -induced and  $\text{Fe}^{3+}$ -induced gels of **1** (top) and SEM images of the metallogels of **1** with  $\text{Fe}^{3+}$  (b and b') and  $\text{Ag}^+$  ions (c and c') (below).

metallogels. The weak emission centered at 434 nm in the sol state suffered a blue shift of 33 nm and 26 nm for the  $\text{Ag}$ -gel and  $\text{Fe}$ -gel, respectively. A new peak at 549 nm for the  $\text{Fe}$ -gel was recorded which could be explained by the overlapping of aromatic units to form a higher array of  $\pi$ - $\pi$  stacking in the gel state. Due to such aggregation, the emission of compound **1** was quenched.

The nature of supramolecular interaction in metallogels of **1** is, however, difficult to predict. We believe that the metal ions possibly coordinate the diazine group in the mode shown in Fig. 5,<sup>5h</sup> and assist the gelators to form a network in solution for gelation. In FTIR, the small decrease in stretching frequency of the imine bonds (from  $1608 \text{ cm}^{-1}$  to  $1606 \text{ cm}^{-1}$ ) during gelation suggested this proposition (Fig. S3, ESI†). Moreover, the shift of stretching of the ester carbonyl in metallogels compared to the amorphous states possible due to involvement in intermolecular connection with the solvent methanol or metal ions could not be ruled out. However, the strong hydrophobic interaction as usually exerted by the cholesteryl surface is presumed to be an additional driving force for aggregation.

The mechanism of interaction was investigated by recording  $^1\text{H}$  NMR of **1** in the absence and presence of these two metal ions (Fig. 5). The presence of  $\text{Ag}^+$  and  $\text{Fe}^{3+}$  ions caused downfield chemical shifts of the imine protons ( $\text{H}_a$ ) by 0.2 ppm and 0.1 ppm, respectively and indicated their small interaction with the diazine group. This metal-ligand interaction also resulted in small downfield chemical shifts of the other aromatic protons ( $\text{H}_b$  and  $\text{H}_c$ ).

### Mechanical properties of the metallogels

To understand the viscoelastic properties of the metallogels, an oscillatory rheological experiment (amplitude sweep and



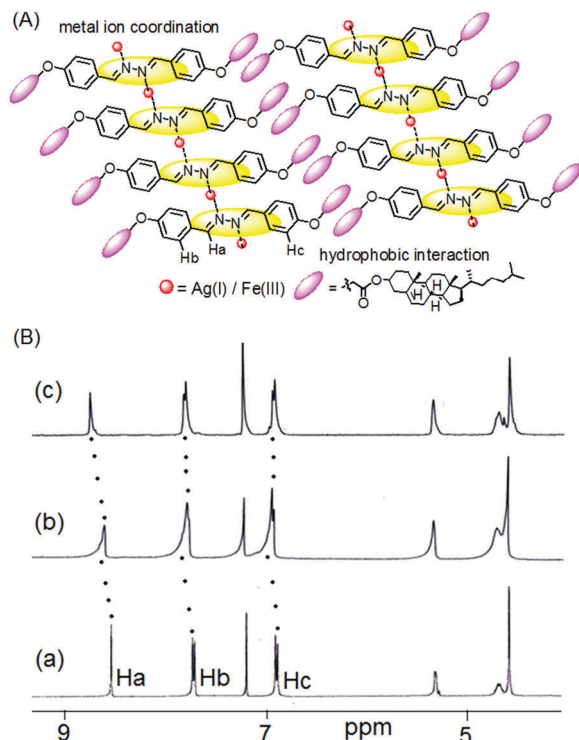


Fig. 5 (A) Probable mode of metal gelator interaction; (B) partial  $^1\text{H}$  NMR spectra of **1** in the absence (a) and presence of an equiv. amount of (b)  $\text{Fe}^{3+}$  and (c)  $\text{Ag}^+$  ions in  $\text{CDCl}_3$ .

frequency sweep) was carried out at  $20^\circ\text{C}$  (Fig. 6). For this experiment, we prepared the gels of **1** upon individual addition of one equiv. amount of  $\text{Ag}^+$  and  $\text{Fe}^{3+}$  ions at their respective 'mgc' values. To find out the linear viscoelastic region, an amplitude sweep experiment of both the gels was carried out at a constant frequency of 1 Hz (Fig. 6a). During this experiment, at lower applied strain, both the elastic/storage modulus ( $G'$ ) and viscous/loss modulus ( $G''$ ) remained almost independent of applied strain (upto almost 1% strain) and displayed strong mechanical behaviour ( $G' \gg G''$ ). However, with gradual increase in applied strain both  $G'$  and  $G''$  were decreased and at a certain strain, crossover between them was noted, above which the viscous property dominates ( $G'' > G'$ ). The crossover points were detected at 6% and 8% of applied strain for the  $\text{Ag}^+$  and  $\text{Fe}^{3+}$ -induced gels, respectively. This indicated disintegration of the respective gels at the applied strain. Demolition of

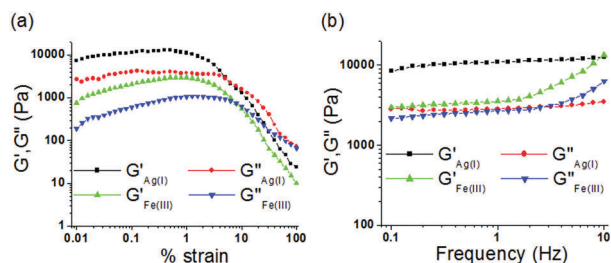


Fig. 6 Rheology experiment of the metallogels of **1**: (a) amplitude sweep and (b) frequency sweep.

Table 1 Summary of rheological properties of the metallogels of **1**

Gel	Strain at crossover (%)	$G'_{av}$ (Pa)	$G''_{av}$ (Pa)	$\tan \delta$ ( $G''_{av}/G'_{av}$ ) <sup>a</sup>
$\text{Ag}^+$ -gel	6	10 280	2823	0.27
$\text{Fe}^{3+}$ -gel	8	3352	2497	0.74

<sup>a</sup> Calculated from frequency sweep data within the linear range of frequency (0.1–1.5 Hz).

the metallogels at lower applied strain (below 10% strain) demonstrated lower strain bearing capability and their fragile nature.<sup>14</sup>

For the gels, during a frequency sweep experiment (at constant strain of 0.5%), the values of  $G'$  were always higher than those of  $G''$  at any frequency which corroborated the true gel nature of the materials (Fig. 6b). For  $\text{Ag}^+$ -gel, both  $G'$  and  $G''$  were frequency independent over the entire range studied (0.1 to 10 Hz), however, at higher frequency (above 1.5 Hz) little frequency dependence of both  $G'$  and  $G''$  was observed for  $\text{Fe}^{3+}$ -gel (frequency hardening as both  $G'$  and  $G''$  increased with increase in applied frequency). Analysis of  $\tan \delta$  values ( $\tan \delta = G''_{av}/G'_{av}$ , 0.27 and 0.74 for the  $\text{Ag}^+$ -gel and  $\text{Fe}^{3+}$ -gel, respectively; Table 1) clearly described the higher mechanical strength (lower  $\tan \delta$ ) of the  $\text{Ag}^+$ -gel in comparison to the  $\text{Fe}^{3+}$ -gel. Most importantly, despite the lower gelator concentration, the  $\text{Ag}^+$ -gel showed almost three times higher storage modulus ( $G'$ ) than the  $\text{Fe}^{3+}$ -gel, thereby indicating its greater stability over the  $\text{Fe}^{3+}$ -gel.<sup>14</sup>

### Metal ion binding study of **1** in solution

The gelator **1** also exhibited measurable interaction in solution. Solution phase interactions were measured by recording UV-vis and fluorescence spectra of compound **1** ( $c = 2.50 \times 10^{-5}$  M) upon adding different metal ions (as perchlorate salts,  $c = 1.0 \times 10^{-3}$  M) in  $\text{CHCl}_3/\text{CH}_3\text{OH}$  (3:1, v/v). During UV-vis titration, addition of  $\text{Ag}^+$  ions (upto 40 equiv.) resulted in a weak ratiometric spectral change in the corresponding absorption spectrum. The initial absorption peak at 326 nm was progressively decreased and two clear isosbestic points at 368 nm and 274 nm were observed (Fig. S4, ESI†). In the case of  $\text{Fe}^{3+}$  ions (upto 40 equiv.), the initial absorption band at 326 nm was gradually increased and red shifted by 13 units (Fig. S4, ESI†). In this change in absorption of **1** at 326 nm, the absorption originated from solvent- $\text{Fe}^{3+}$  ion interaction may remain interweaved as confirmed from Fig. S5 (ESI†). All other metal ions did not bring similar spectral changes under these conditions (Fig. S5, ESI†).

Although compound **1** does not have any fluorescent probe, it on examination showed selective interaction in fluorescence towards  $\text{Fe}^{3+}$  ions only. Fig. 7a, in this regard, displays the change in fluorescence ratio ( $\lambda_{\text{ex}} = 330$  nm) at 434 nm upon addition of 30 equiv. amounts of different metal ions. Addition of  $\text{Fe}^{3+}$  ions resulted in significant quenching of emission at 434 nm (Fig. 7b), whereas all other metal ions remained non-interacting in the study (Fig. 7c). The fluorescence quenching of **1** in the presence of  $\text{Fe}^{3+}$  ions was possibly attributed to the heavy atom effect of  $\text{Fe}^{3+}$  ions.<sup>11b</sup>

The Benesi-Hildebrand plot<sup>15</sup> indicated linear binding of **1** with both  $\text{Fe}^{3+}$  and  $\text{Ag}^+$  ions. The corresponding binding

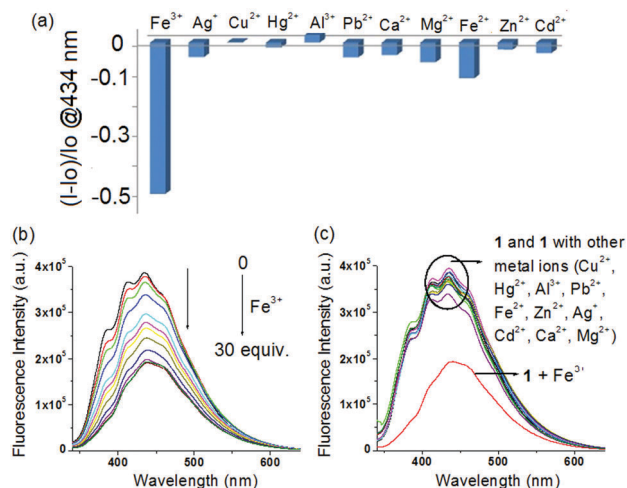


**Fig. 7** (a) Change in fluorescence ratio ( $I_{\text{ex}} = 330 \text{ nm}$ ) of **1** ( $c = 2.5 \times 10^{-5} \text{ M}$ ) at 434 nm upon addition of 30 equiv. amounts of different metal ions ( $c = 1.0 \times 10^{-3} \text{ M}$ ) in  $\text{CHCl}_3/\text{CH}_3\text{OH}$  (3:1, v/v); change in fluorescence intensity of **1** upon addition of 30 equiv. amounts of (b)  $\text{Fe}^{3+}$  and (c) different metal ions.

constant values and detection limit<sup>16</sup> (Fig. S6–S8, ESI<sup>†</sup>) were calculated (Table S2, ESI<sup>†</sup>). The detection limits were obtained as  $9.35 \times 10^{-6} \text{ M}$  and  $5.85 \times 10^{-5} \text{ M}$ , for  $\text{Ag}^+$  and  $\text{Fe}^{3+}$  ions, respectively. Thus compound **1** could serve as an LMWG for the selective and differential recognition of  $\text{Fe}^{3+}$  and  $\text{Ag}^+$  ions, in a gel state as well as in the solution phase.

### Non interference of $\text{Fe}^{2+}$ ions during $\text{Fe}^{3+}$ sensing and detection of *in situ* generated $\text{Fe}^{3+}$ ions

We were eager to examine the interference of  $\text{Fe}^{2+}$  ions during a  $\text{Fe}^{3+}$  sensing process. In this case, we observed that  $\text{Fe}^{3+}$ -induced gelation could also be achieved in the presence of  $\text{Fe}^{2+}$  ions (Fig. 8A). When  $\text{Fe}^{3+}$  ions were added to  $\text{Fe}^{2+}$ -containing sol of **1**, orange colored gel formation was noticed. This study primarily established the non interference of  $\text{Fe}^{2+}$  ions during  $\text{Fe}^{3+}$ -promoted gelation.

As compound **1** can discriminate  $\text{Fe}^{3+}$  ions from  $\text{Fe}^{2+}$  ions in the gel phase, we further investigated its practical application in detecting *in situ* generated  $\text{Fe}^{3+}$  ions. A thorough experiment, in this regard, is represented in Fig. 8A. First, the gelation of compound **1** was investigated either in the presence of  $\text{Fe}^{2+}$  ions or *m*-chloroperbenzoic acid (*m*CPBA), an oxidizing agent. In both cases, we obtained solutions. However, addition of *m*CPBA to the  $\text{Fe}^{2+}$  containing sol of **1** brought gelation. Gelation also took place in the reverse way when  $\text{Fe}^{2+}$  ions were added to a solution of **1** containing *m*CPBA.

The *in situ* generation of  $\text{Fe}^{3+}$  ions in the presence of *m*CPBA, actually caused gelation of **1**. This was further established by  $^1\text{H}$  NMR. The  $^1\text{H}$  NMR spectrum of **1** in  $\text{CDCl}_3$  remained almost unperturbed either in the presence of *m*CPBA or in the presence of  $\text{Fe}^{2+}$ . However, addition of  $\text{Fe}^{2+}$  ions to an *m*CPBA containing solution of **1** caused downfield chemical shift of the imine protons by 0.1 units ( $\text{H}_a$ , from 5.53 ppm to 5.64 ppm, Fig. 8B). A similar downfield chemical shift of  $\text{H}_a$  protons was observed

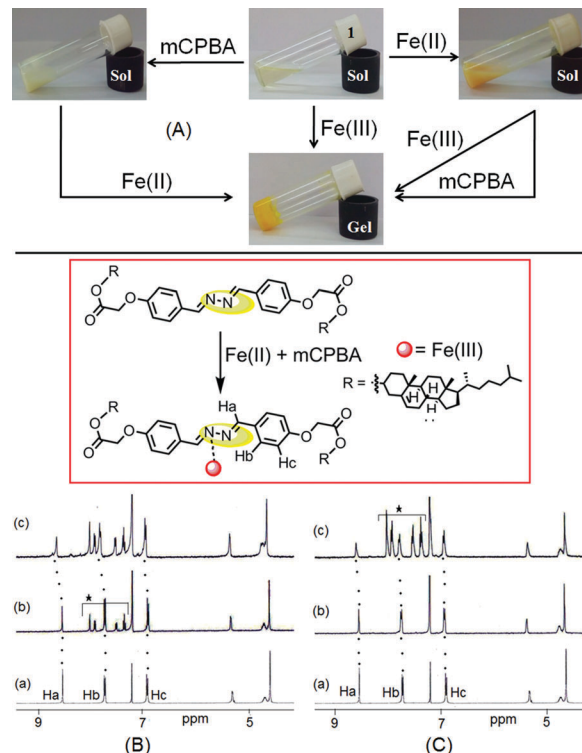


**Fig. 8** (A) Photograph showing the responsiveness of **1** in  $\text{CHCl}_3/\text{CH}_3\text{OH}$  (3:1, v/v) with  $\text{Fe}^{2+}$ ,  $\text{Fe}^{3+}$  and *m*CPBA under different conditions [in the study, an equiv. amount of  $\text{Fe}^{3+}$  and  $\text{Fe}^{2+}$  ions, and 2 equiv. amount of *m*CPBA as an oxidant were used], (B) partial  $^1\text{H}$  NMR spectra of (a) **1**, (b) **1** with *m*CPBA and (c) **1** with *m*CPBA followed by addition of  $\text{Fe}^{2+}$  (as perchlorate salt), (C) partial  $^1\text{H}$  NMR spectra of (a) **1**, (b) **1** with  $\text{Fe}^{2+}$  (as perchlorate salt) and (c) **1** with  $\text{Fe}^{2+}$  followed by addition of *m*CPBA. NMR studies were carried out in  $\text{CDCl}_3$  with an equiv. amount of different analytes and the asterisk protons in the spectra represent the signals of *m*CPBA.

when *m*CPBA was added to the solution of **1** containing  $\text{Fe}^{2+}$  ions (Fig. 8C). In addition to positional movement of the imine protons, the signals for  $\text{H}_b$  and  $\text{H}_c$  moved downfield. The spectral shifts were alike to the case shown in Fig. 5. These results undoubtedly corroborated the *in situ* oxidation of  $\text{Fe}^{2+}$  into  $\text{Fe}^{3+}$  and its subsequent participation in the gelation of **1**. A similar *in situ* oxidation of  $\text{Fe}^{2+}$  using  $\text{H}_2\text{O}_2$  was unsuccessful.

In practice, most of the  $\text{Fe}^{3+}$ -sensing probes suffer from interference from  $\text{Fe}^{2+}$  ions.<sup>10c-f</sup> Even gel phase detection of  $\text{Fe}^{3+}$  ions also experiences such interference.<sup>11a</sup> However, some reported studies have not included the effect of  $\text{Fe}^{2+}$  ions during  $\text{Fe}^{3+}$  ion sensing.<sup>11b</sup> So, development of an efficient sensing probe for  $\text{Fe}^{3+}$  ions having no interference from  $\text{Fe}^{2+}$  ions is a great challenge. In this scenario, our present gelator structure **1** demands merit as a sensor for detection of  $\text{Fe}^{3+}$  ions even in the presence of  $\text{Fe}^{2+}$  ions in a sol-gel method.

### Application of the metallogels

(a) **In discrimination of halides.** The metallogels were explored as soft functional materials for visual discrimination of different halides (Fig. S9, ESI<sup>†</sup>). We have earlier shown in Fig. 3b that addition of  $\text{TBACl}$  to the  $\text{Ag}^+$ -induced gel could

influence the gel state of **1**, causing complete destruction of the gel, whereas the  $\text{Fe}^{3+}$ -induced gel remained intact under identical conditions. Interestingly, all other halides (TBAF, TBABr and TBAI) were unable to produce such gel-sol phase transformation of the  $\text{Ag}^+$ -induced gel. These observations are useful in visual discrimination of chloride ions from other halides.

On the other hand, both TBAF and TBABr ruptured the  $\text{Fe}^{3+}$ -induced gel and resulted in respective sols of yellow and orange-red color. In this event, TBAI remained silent in such phase changes although the color of the  $\text{Fe}^{3+}$ -gel became orange-red from orange. All these results are declared to be useful in visual recognition and discrimination of the halides from each other.

**(b) In dye adsorption.** Apart from sensing and recognition, for additional practical utility of **1**, we further explored the metallogels of **1** in dye adsorption. In practice, dyes have wide industrial usages as colouring agents.<sup>17</sup> However, they are toxic to humans and aquatic organisms, and therefore, removal of dyes from water is worth mentioning. Regarding this, the use of LMWGs as potential dye adsorbents has grown enormously in the last few decades.<sup>18</sup> In this situation, it is important to note that the presence of a large hydrophobic surface in a gelator structure is often found to have a pronounced impact in the adsorption of dyes in the aggregated state.

We investigated the dye adsorption efficiency of  $\text{Fe}^{3+}$ - and  $\text{Ag}^+$ -induced gels of **1** towards anionic dye uranine. Recently, Thomas *et al.* demonstrated the adsorption of oppositely charged dyes by a cross-linked hydrogel and showed that selective adsorption of dyes predominantly depends upon the electrostatic interaction between the hydrogel and dyes.<sup>18c</sup> Regarding this, we assumed that the electrostatic interaction between the metal ion of gels and uranine would be beneficial for the successful and efficient adsorption of the anionic dye uranine on the cholesteryl hydrophobic surfaces. Furthermore, depending upon the charge-charge interaction, different efficacy of the  $\text{Fe}^{3+}$ - and  $\text{Ag}^+$ -metallogels towards uranine adsorption could easily be anticipated.

To execute these features, first we examined the feasibility of adsorption on the metallogels by preparing the respective metallogels in the presence of uranine in  $\text{CHCl}_3/\text{CH}_3\text{OH}$  (3:1, v/v). Importantly, in both cases, stable gels were obtained (Fig. 9, top). These results suggested that the gels retained their aggregated structure even in the presence of uranine.

To perform the dye adsorption experiment, we placed  $\text{Fe}^{3+}$ - and  $\text{Ag}^+$ -gels of **1**, separately into vials containing aqueous uranine solution (3 mL). After separation of the respective dye adsorbed gels from the aqueous parts through filtration, the efficiency of the gels as dye adsorbents was measured by recording the absorption spectra of the dye solutions before and after the addition of the gels. Fig. 9 and 10 and Table 2, in this regard, represent the details along this direction.

To confirm the uranine adsorption, FTIR and UV-vis spectra of the respective metallogels were compared before and after the adsorption process. In FTIR, the presence of the characteristic stretching signals of both **1** and uranine (with some variations in peak positions) in both the dye-adsorbed gels verified the adsorption (Fig. S10, ESI†). Furthermore, for the

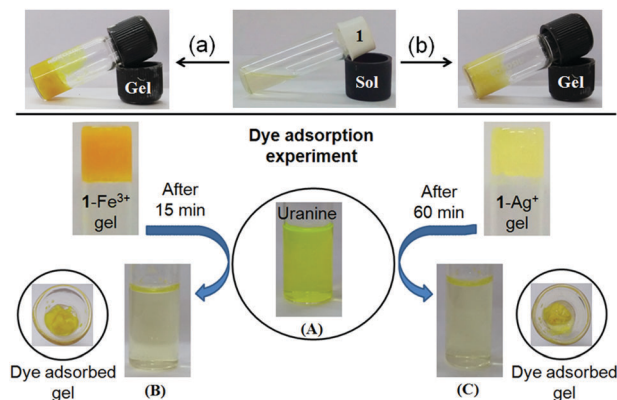


Fig. 9 Photograph representing the gel formation of **1** in  $\text{CHCl}_3/\text{CH}_3\text{OH}$  (3:1, v/v) upon simultaneous addition of (a)  $\text{Fe}^{3+}$  and uranine and (b)  $\text{Ag}^+$  and uranine [uranine solution was prepared in MeOH containing a few drops of water] (top), photograph showing the adsorption of uranine ( $c = 3 \times 10^{-5}$  M) by **1**- $\text{Fe}^{3+}$  gel (A  $\rightarrow$  B) and **1**- $\text{Ag}^+$  gel (A  $\rightarrow$  C). The gels were initially prepared by adding an equiv. amount of respective metal salts to **1** ( $25 \text{ mg mL}^{-1}$ ) in  $\text{CHCl}_3/\text{CH}_3\text{OH}$  (3:1, v/v) (bottom).

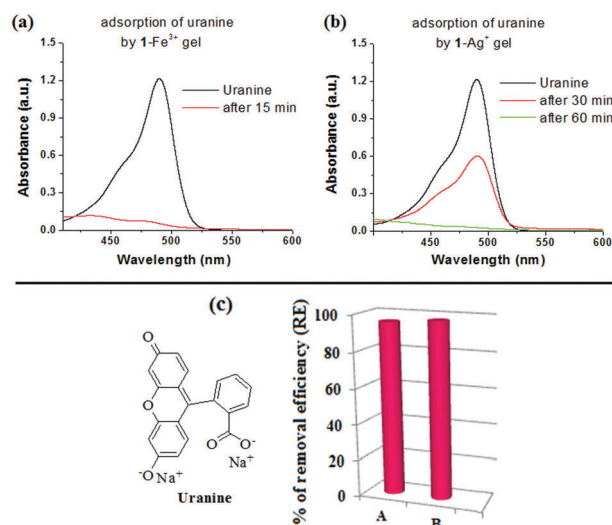


Fig. 10 Change in absorbance of uranine solution ( $c = 3 \times 10^{-5}$  M) before and after adsorption on (a) **1**- $\text{Fe}^{3+}$  gel and (b) **1**- $\text{Ag}^+$  gel. (c) The bar plot shows the respective dye adsorption data; adsorption of uranine by (A) **1**- $\text{Fe}^{3+}$  and (B) **1**- $\text{Ag}^+$  gels.

dye-adsorbed gels, the presence of strong absorption bands in the region 440–490 nm (for uranine) established the successful adsorption (Fig. 11a and b). Such spectral appearance of the absorption bands of uranine was due to metal-uranine interaction. Spectral matches confirmed this attribute (Fig. S11, ESI†).

The used gelator in adsorption was recovered by washing the dye adsorbed gel with aqueous MeOH (1:1 v/v) and demonstrated the recyclability of the process (Fig. 11c).

The rapid removal of uranine by **1**- $\text{Fe}^{3+}$  gel, in comparison to **1**- $\text{Ag}^+$  gel, is certainly due to electrostatic interaction where a higher charge density in **1**- $\text{Fe}^{3+}$  gel preferentially exerts strong nucleophilic-electrophilic interaction. Moreover, in our opinion the porous gel architecture of **1**- $\text{Fe}^{3+}$  gel, in contrast to the



Table 2 Summary of adsorption data for the metallogels of **1** using uranine dye

Dye ( $\lambda_{\text{max}}$ in nm)	Gel	Initial conc. of the dye ( $C_i$ ) [mM] (mg L <sup>-1</sup> )	Equilibrium conc. of the dye ( $C_e$ ) [mM] (mg L <sup>-1</sup> )	Quantity of the adsorbed dye (mg per gram of the gelator) <sup>a</sup>
Uranine (490)	1-Fe <sup>3+</sup>	$3 \times 10^{-2}$ (10.59)	$1.31 \times 10^{-3}$ (0.46)	1215
	1-Ag <sup>+</sup>		$7.40 \times 10^{-4}$ (0.26)	1239

<sup>a</sup> Calculations are made on the basis of absorption spectral changes in PA solution after 15 min and 1 h for 1-Fe<sup>3+</sup> and 1-Ag<sup>+</sup> gel, respectively.

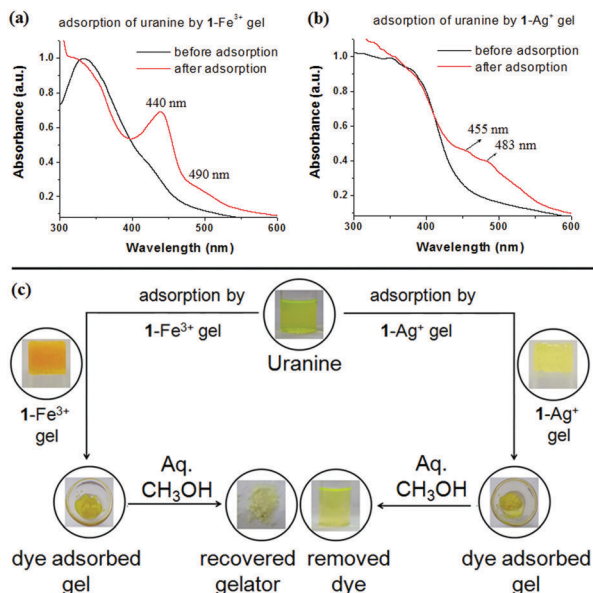


Fig. 11 Comparison of normalized UV-vis spectra of (a) 1-Fe<sup>3+</sup> gel and (b) 1-Ag<sup>+</sup> gel, before and after adsorption of uranine and (c) photograph showing the recyclability of the uranine adsorption process.

globular microstructured 1-Ag<sup>+</sup> gel, additionally favors faster adsorption. This observation has relevance in real life as the response time is short compared to other reported gels that usually take a couple of hours to perform the process.<sup>1g,17</sup>

(c) **In picric acid (PA) removal from water.** Prolific use of the metallogels as potential dye adsorbents encouraged us to explore the gels as soft materials towards picric acid adsorption from water. Among the common nitroaromatics, PA is considered as a stronger explosive than its well known counterpart trinitrotoluene (TNT) and has widely been used as a primary constituent of many explosives and landmines.<sup>19</sup> However, because of its high water solubility, excessive exposure of PA contaminates water and soil and causes serious health effects.<sup>20</sup> Sensing and detection of PA is therefore a promising research area concerning security and environmental issues. Several attempts, in this regard, have been made to develop fluorogenic chemosensors as well as LMWGs for selective sensing and recognition of PA.<sup>21</sup> However, the application of LMWGs in water treatment for adsorption and removal of PA is rare.<sup>21a</sup> It is further mentionable that owing to the high solubility of PA in water, it is very difficult to separate it from contaminated water sources. Thus the design of LMWGs as a useful material for sensing and removal of PA from water has strong relevance from physiological and environmental points of view.

Prior to investigating the PA removal from water, we examined the stability of the metallogels in the presence of PA. No visual changes of the gel states were detected upon addition of an equiv. amount of PA to the gels. Importantly, when we prepared the metallogels in the presence of both PA and respective metal ions in CHCl<sub>3</sub>/CH<sub>3</sub>OH (3 : 1, v/v), in each case instant gelation occurred (Fig. S12, ESI<sup>†</sup>). This established the sustainability of the metallogels in the presence of PA.

A PA adsorption experiment was carried out according to the same procedure as followed for a dye adsorption experiment. The Fe<sup>3+</sup>- and Ag<sup>+</sup>-gels of **1** were separately placed into the aqueous solutions of PA (3 mL). To evaluate the PA removal efficiency of the metallogels, change in absorption of the PA solution was monitored with time. The detailed experiment is shown in Fig. 12 and the outcomes are summarised in Table 3.

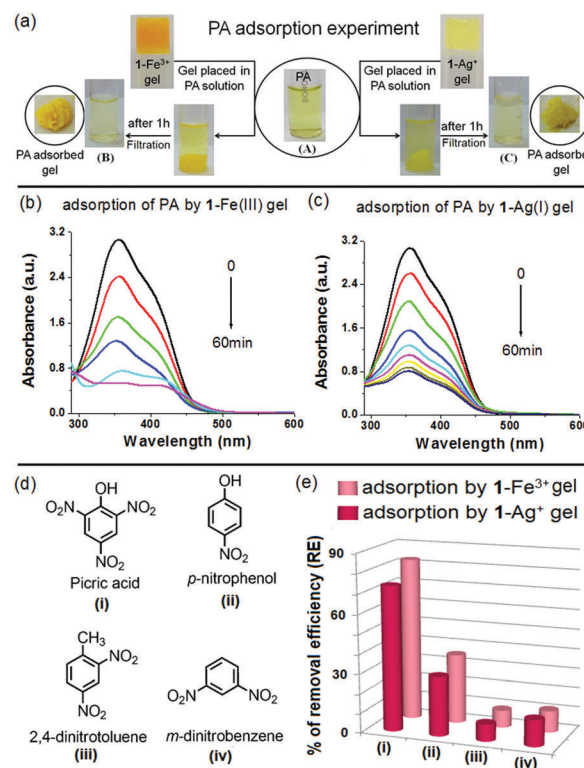


Fig. 12 (a) Photograph showing the adsorption of PA (3 mL in water, c = 2 × 10<sup>-4</sup> M) by 1-Fe<sup>3+</sup> gel (A → B) and 1-Ag<sup>+</sup> gel (A → C), change in absorbance of PA solution during adsorption by (b) 1-Fe<sup>3+</sup> and (c) 1-Ag<sup>+</sup> gels, (d) structures of the nitroaromatic compounds and (e) bar plot showing their % of adsorption by the 1-Fe<sup>3+</sup> and 1-Ag<sup>+</sup> gels after 1 h [For m-dinitrobenzene, c = 1 × 10<sup>-4</sup> M; for other cases, c = 2 × 10<sup>-4</sup> M; the gels were initially prepared by adding an equiv. amount of the respective metal salt to **1** (25 mg mL<sup>-1</sup>) in CHCl<sub>3</sub>/CH<sub>3</sub>OH (3 : 1, v/v)].

Table 3 Summary of adsorption data for the metallogels of **1** using PA

Gel	Initial conc. of PA ( $C_i$ ) [mM] ( $\text{mg L}^{-1}$ )	Equilibrium conc. of PA ( $C_f$ ) [mM] ( $\text{mg L}^{-1}$ )	Quantity of the adsorbed PA (mg per gram of the gelator)
<b>1-Fe<sup>3+</sup></b>	$2 \times 10^{-1}$ (45.82)	$3.4 \times 10^{-2}$ (7.94)	4546
<b>1-Ag<sup>+</sup></b>		$5.2 \times 10^{-2}$ (11.96)	4063

Both the metallogels showed measurable efficiency towards removal of PA. Almost 83% and 74% adsorptions were noticed with the **1-Fe<sup>3+</sup>** and **1-Ag<sup>+</sup>** gels, respectively in 1 h (Fig. 12a–c). In comparison, both the metallogels showed very small extent of adsorption for the nitroaromatics having either no phenol –OH or fewer nitro groups (Fig. 12d and e). Negligible adsorption was recorded for simple nitroaromatics without phenolic –OH (8.76% and 8.88% for 2,4-dinitrotoluene and 13.58% and 11.11% *m*-dinitrobenzene by **1-Ag<sup>+</sup>** and **1-Fe<sup>3+</sup>** gel, respectively) (Fig. 12e and Fig. S13, ESI†). Adsorption was moderate for *p*-nitrophenol (30.29% and 35.45% by **1-Ag<sup>+</sup>** and **1-Fe<sup>3+</sup>** gel, respectively) (Fig. 12e and Fig. S13, ESI†). Efficient removal of PA by the metallogels is presumably due to strong interaction of the phenolic –OH of PA with the metal ions of the gel matrixes and in this context, the **1-Fe<sup>3+</sup>** gel is better than the **1-Ag<sup>+</sup>** gel.

Comparison of FTIR and UV-vis spectra of the PA adsorbed gels with the pristine metallogels unequivocally established the successful adsorption phenomena. FTIR spectra of the PA adsorbed gels exhibited characteristic stretching signals of both the gelators and PA (Fig. S14, ESI†). The characteristic absorption band of PA was also found in the PA adsorbed gels (350–426 nm region, Fig. S15, ESI†). These peaks were absent in the mother metallogels. Here also, washing of the PA adsorbed gels with aqueous MeOH afforded the gelator back for reuse (Fig. S16, ESI†).

In reality, in spite of the large volume of studies on PA-responsive supramolecular gelators, the successful use of LMWGs as PA adsorbents with high removal efficacy in a short response time is rare. Recently, Cao *et al.* reported the adsorption of PA by a pyridine coupled naphthalimide-based gelator with moderate efficiency even after a day of performance (from absorption spectroscopic study, only 56.86% removal of PA was reported in 24 h).<sup>21a</sup> In this situation, this present work provides a new insight into fabricating new metallo–organic gel matrixes (MOG) for efficient removal of PA from water.

## Conclusions

In conclusion, we have established that the diazine unit as a metal binding site in our designed structure **1** is unique in gel chemistry with various applications. Gelator **1** forms nice gels in the presence of Fe<sup>3+</sup> and Ag<sup>+</sup> ions in CHCl<sub>3</sub>/CH<sub>3</sub>OH mixture solvent. It is important to note that although a reasonable number of fluorescent probes for Fe<sup>3+</sup> and Ag<sup>+</sup> ions are known in the literature, until now, reports of the gel phase sensing of these metal ions are less in number, and in particular Fe<sup>3+</sup> ion responsive LMWGs are very rare. Importantly, most of the sensing probes for Fe<sup>3+</sup> ions (chemosensors as well as gelators) usually experience the interference of Fe<sup>2+</sup> ions. A comparative

view on this is represented in Table S3 (ESI†). In comparison, this present report receives attention as the gelator **1** does not experience any interference from Fe<sup>2+</sup> ions during Fe<sup>3+</sup>-sensing, although response from Ag<sup>+</sup> ions was observed. However, TBACl, TBAF and NH<sub>4</sub>SCN successfully discriminate Fe<sup>3+</sup>- and Ag<sup>+</sup>- metallogels.

Both the metallogels reveal fibrillar to globular porous microstructures as confirmed from SEM images. The true nature of the gels has been realized from a rheological study in detail. The study indicates that despite the lower gelator concentration, the Ag<sup>+</sup>-gel shows almost three times higher storage modulus ( $G'$ ) than the Fe<sup>3+</sup>-gel, thereby highlighting its greater stability over the Fe<sup>3+</sup>-gel. Owing to the presence of metal ions, both the gels show adsorption characteristics. Uracine and picric acid are efficiently adsorbed from water. In this process, the metallogels are recyclable and exhibit excellent efficiency. These properties of the metallogels, which are rarely discussed in the literature (Table S4, ESI†), draw much attention concerning the practical point of view in the present report. Further investigations in this direction are underway in our laboratory.

## Experimental

### Materials and methods

All the chemicals and reagents were purchased from Spectrochem, India. Perchlorate salts of the metal ions were purchased from Sigma-Aldrich and were carefully handled. All solvents used in the synthesis were purified, dried and distilled as required. Solvents used in NMR experiments were obtained from Aldrich. Thin layer chromatography was performed on Merck precoated silica gel 60-F<sub>254</sub> plates. <sup>1</sup>H and <sup>13</sup>C NMR spectra were recorded using a Bruker 400 MHz instrument using TMS as an internal standard. High resolution mass data were acquired by the electron spray ionization (ESI) technique on an XEVO GS-2 QTOF Waters mass spectrometer. FTIR measurements of the compounds were carried out using a Perkin-Elmer L120-00A spectrometer ( $\nu_{\text{max}}$  in cm<sup>−1</sup>) using KBr pellets. Fluorescence and UV-vis studies were performed using a Horiba Fluoromax 4C spectrofluorimeter and Shimadzu UV-2450 spectrophotometer, respectively.

### Synthesis and characterization

**Compound 2<sup>4</sup>.** To a stirred solution of cholesterol (0.5 g, 1.29 mmol) in 20 mL dry CHCl<sub>3</sub> was added chloroacetyl chloride (0.16 mL, 1.93 mmol) and pyridine (0.05 mL, 0.65 mmol) under a nitrogen atmosphere. The mixture was allowed to stir for 10 h at room temperature. After completion of the reaction, the reaction mixture was neutralized with NaHCO<sub>3</sub> solution, and then was extracted with CHCl<sub>3</sub> (3 × 30 mL). The organic layer was



washed several times with water and separated and dried over  $\text{Na}_2\text{SO}_4$ . Evaporation of the solvent gave a white solid compound. Recrystallization from  $\text{CH}_3\text{OH}$  afforded pure product **2** (0.58 g, yield 96%, m.p. 148 °C).  $^1\text{H}$  NMR (400 MHz,  $\text{CDCl}_3$ ):  $\delta$  5.37 (m, 1H), 4.72 (m, 1H), 4.03 (s, 2H), 2.36 (m, 2H), 2.02–0.85 (m, 38H, cholesteryl protons), 0.67 (s, 3H); FTIR (KBr,  $\text{cm}^{-1}$ ): 2939, 2907, 2821, 1753, 1620, 1195.

**Compound 3**<sup>4</sup>. A mixture of 4-hydroxy benzaldehyde (1 g, 8.19 mmol) and  $\text{K}_2\text{CO}_3$  (2.26 g, 16.38 mmol) was refluxed in dry  $\text{CH}_3\text{CN}$  for 2 h and then compound **2** (4.55 g, 9.82 mmol) was added to it. The reaction mixture was refluxed for 5 h. Then the organic solvent was evaporated under reduced pressure and water was added to the crude mass. Then reaction mixture was extracted with 2%  $\text{CH}_3\text{OH}$  in  $\text{CHCl}_3$ . Evaporation of the solvent gave the crude product which was purified by column chromatography using 10% ethyl acetate in petroleum ether as an eluent to afford the pure compound **3** in 78% yield (3.50 g, m.p. 114 °C).  $^1\text{H}$  NMR ( $\text{CDCl}_3$ , 400 MHz):  $\delta$  9.90 (s, 1H), 7.85 (d, 2H,  $J = 8$  Hz), 7.01 (d, 2H,  $J = 8$  Hz), 5.38 (d, 1H,  $J = 4$  Hz), 4.75 (m, 1H), 4.68 (s, 2H), 2.35–0.67 (43H, cholesteryl protons);  $^{13}\text{C}$  NMR ( $\text{CDCl}_3$ , 100 MHz):  $\delta$  190.7, 167.5, 162.6, 139.0, 131.9, 130.6, 123.2, 114.9, 75.6, 65.3, 56.6, 56.1, 49.9, 42.3, 39.6, 39.5, 37.9, 36.8, 36.5, 36.1, 35.7, 31.89, 31.82, 29.7, 28.2, 28.0, 27.6, 24.2, 23.8, 22.8, 22.5, 21.0, 19.2, 18.7, 11.8; FTIR (KBr)  $\nu$   $\text{cm}^{-1}$ : 3403, 2945, 1775, 1701, 1606, 1212; HRMS (TOF MS  $\text{ES}^+$ ): calcd 549.3866 ( $\text{M} + 1$ )<sup>+</sup>, found 549.3890 ( $\text{M} + 1$ )<sup>+</sup>.

**Compound 1**. Compound **3** (1.0 g, 1.82 mmol) and  $\text{N}_2\text{H}_4 \cdot \text{H}_2\text{O}$  (0.04 g, 0.91 mmol) were taken in 20 mL dry benzene and refluxed for 3 days. After that, benzene was evaporated and the reaction mixture was repeatedly washed with MeOH to have the pure compound **1** in appreciable yield (0.72 g, yield 82%, m.p. 234 °C).  $^1\text{H}$  NMR (400 MHz,  $\text{CDCl}_3$ ):  $\delta$  8.53 (s, 2H), 7.71 (d, 4H,  $J = 8$  Hz), 6.89 (d, 4H,  $J = 8$  Hz), 5.32 (d, 2H,  $J = 4$  Hz), 4.68 (m, 2H), 4.58 (s, 4H), 2.29–0.67 (86H, cholesteryl protons);  $^{13}\text{C}$  NMR (100 MHz,  $\text{CDCl}_3$ ):  $\delta$  167.9, 161.0, 160.1, 139.1, 130.1, 127.8, 123.1, 114.9, 75.4, 65.4, 56.6, 56.1, 49.9, 42.3, 39.6, 39.5, 37.9, 36.8, 36.5, 36.1, 35.8, 31.89, 31.82, 28.2, 28.0, 27.6, 24.2, 23.8, 22.8, 22.5, 21.0, 19.3, 18.7, 11.8; FTIR (KBr,  $\text{cm}^{-1}$ ): 2946, 1768, 1608, 1510; HRMS (TOF MS  $\text{ES}^+$ ): calcd 1092.7894 ( $\text{M}$ )<sup>+</sup>, found 1092.7826 ( $\text{M}$ )<sup>+</sup>.

### General procedure for a gelation test

The required amount of compound **1** was taken in the desired solvent (1 mL), slightly warmed to form a homogeneous solution and then allowed to cool to room temperature to form a gel. Stimuli responsive behaviour of the gel was investigated in the presence of different analytes in the same way.  $\text{AgNO}_3$  solution was prepared in  $\text{CH}_3\text{OH}$  containing 0.01%  $\text{H}_2\text{O}$  and  $\text{Fe}(\text{NO}_3)_3$  solution was prepared in MeOH. The gels were tested via the usual inversion of the vial method. Samples of gels for SEM imaging were dried under vacuum and then coated with a thin layer of gold metal. The gel-to-sol transition temperature ( $T_{\text{gel}}$ ) was measured by the dropping ball method.

### General procedure for fluorescence and UV-vis titrations

A stock solution of the compound **1** was prepared in  $\text{CHCl}_3/\text{CH}_3\text{OH}$  (3:1, v/v) in the concentration range of  $10^{-5}$  M.

Stock solutions of cations were prepared in the same solvent in the concentration range of  $10^{-3}$  M. The solution of the compound (2 mL) was taken in the cuvette and to the solution different metal ions were individually added in different amounts. Upon addition of metal ions, the changes in emission of the compound were recorded. The same stock solutions were used for the UV-vis titration experiment in the same way.

### Binding constant determination<sup>15</sup>

A Benesi–Hildebrand plot was adopted to determine the binding constant value using the expression:  $I_0/(I - I_0) = [\epsilon_{\text{M}}/(\epsilon_{\text{M}} - \epsilon_{\text{C}})](K_{\text{a}}^{-1} C_{\text{g}}^{-1} + 1)$ , where  $\epsilon_{\text{M}}$  and  $\epsilon_{\text{C}}$  represent molar extinction coefficients for the receptor structure **1** and the complex, respectively, at a selected wavelength,  $I_0$  denotes the emission intensity of the free receptor structure **1** at that specific wavelength and  $C_{\text{g}}$  is the concentration of the metal ion. The measured absorbance  $I_0/(I - I_0)$  as a function of the inverse of the metal ion concentration fits a linear relationship, indicating 1:1 stoichiometry of the receptor **1**–metal ion complex. The ratio of the intercept to the slope was used to determine the binding constant  $K_{\text{a}}$ . Instead of fluorescence intensities, respective absorbance of the receptor structure was also used to get the binding constant values.

### Calculation of detection limit<sup>16</sup>

The detection limit was calculated using the fluorescence and UV-vis titration data. The emission and absorbance of **1** were measured 5 times, and the standard deviation of a blank measurement was achieved. To have the slope, emission intensities and absorbance values were plotted against concentrations of metal ions. The detection limits were calculated using the equation: detection limit =  $3\sigma/k$ , where  $\sigma$  is the standard deviation of the blank measurement, and  $k$  is the slope.

### Dye adsorption experiment<sup>18</sup>

For this study, the gel of **1** [ $25 \text{ mg mL}^{-1}$ ] was prepared in  $\text{CHCl}_3/\text{CH}_3\text{OH}$  (3:1, v/v) solvent in the presence of an equiv. amount of  $\text{Ag}^+$  and  $\text{Fe}^{3+}$  ions. Uranine solution was prepared in the concentration of  $c = 3 \times 10^{-5}$  M in water. The dye removal efficiency (RE) of the gel phase from its aqueous solution (2 mL) was estimated using UV-vis spectroscopy (at 490 nm). The final concentration of the dye in solution was calculated according to the Beer–Lambert law ( $A = \epsilon cl$ ,  $A$  is the absorbance of the dye at a certain absorption wavelength in solution,  $\epsilon$  is the molar extinction coefficient and  $l$  is the path length of the incident light), which ultimately determined the removal efficiency of the dye via the equation:  $\text{RE} = (C_i - C_f)/C_i$ , in which  $C_i$  represents the initial concentration of the dye in solution;  $C_f$  is the final concentration of the dye in the presence of adsorbing gel.

### Picric acid (PA) adsorption experiment<sup>18</sup>

For this study, the gel of **1** [ $25 \text{ mg mL}^{-1}$ ] was prepared in  $\text{CHCl}_3/\text{CH}_3\text{OH}$  (3:1, v/v) solvent in the presence of an equiv. amount of  $\text{Ag}^+$  and  $\text{Fe}^{3+}$  ions. Solutions of PA and other nitroaromatic compounds (3 mL) were prepared in the concentration  $c = 2 \times 10^{-4}$  M, and for *m*-dinitrobenzene,  $c = 1 \times 10^{-4}$  M.

PA solution was prepared in pure water, while for other cases aqueous solutions containing 0.01% CH<sub>3</sub>CN were used for a clear solution. The removal efficiency (RE) of PA from its aqueous solution (2 mL) was estimated using UV-vis spectroscopy (at 354 nm), as described for the uranine adsorption experiment.

### General statement on recyclability of the adsorption process using the metallogels

The metallogels as used in the adsorption process (dye/PA) were reusable with modification. The compound as isolated in the way mentioned in the text was unable to form a gel under the prescribed conditions and therefore, it was difficult to use directly in the next cycle. The non gelation indicated either the absence or inappropriate amount of metal ions (Fe<sup>3+</sup>/Ag<sup>+</sup>) in the isolated gelator. However, addition of the required amount of the metal salts (Fe<sup>3+</sup>/Ag<sup>+</sup>) to the recovered gelator furnished an instant gel which can be reused successfully in the adsorption process.

## Conflicts of interest

There are no conflicts to declare.

## Acknowledgements

AP thanks CSIR, New Delhi, India for a fellowship. KG thanks SERB, DST, New Delhi, for financial support (File no. EMR/2016/008005/OC).

## References

- (a) J. W. Steed, *Chem. Soc. Rev.*, 2010, **39**, 3686; (b) M.-O. Piepenbrock, G. O. Lloyd, N. Clarke and J. W. Steed, *Chem. Rev.*, 2010, **110**, 1960; (c) A. Y.-Y. Tam and V. W.-W. Yam, *Chem. Soc. Rev.*, 2013, **42**, 1540; (d) H. Maeda, *Chem. – Eur. J.*, 2008, **14**, 11274; (e) K. Ghosh, A. Panja and S. Panja, *New J. Chem.*, 2016, **40**, 3476; (f) S. Panja, S. Bhattacharya and K. Ghosh, *Mater. Chem. Front.*, 2018, **2**, 385; (g) S. Panja, S. Bhattacharya and K. Ghosh, *Langmuir*, 2017, **33**, 8277; (h) S. Panja, S. Ghosh and K. Ghosh, *New J. Chem.*, 2018, **42**, 6488; (i) A. Panja and K. Ghosh, *ChemistrySelect*, 2018, **3**, 1809; (j) A. Panja and K. Ghosh, *Mater. Chem. Front.*, 2018, **2**, 186; (k) A. Panja and K. Ghosh, *ChemistrySelect*, 2018, **3**, 9448.
- (a) R. G. Weiss and P. Terech, *Molecular Gels*, Springer, Dordrecht, 2006, p. 978; (b) F. Fages, *Low Molecular Mass Gelators, Topics in Current Chemistry*, Springer-Verlag, Berlin, 2005, **256**, p. 283; (c) S. S. Babu, V. K. Praveen and A. Ajayaghosh, *Chem. Rev.*, 2014, **114**, 1973; (d) P. A. Gale, N. Busschaert, C. J. E. Haynes, L. E. Karagiannidis and I. L. Kirby, *Chem. Soc. Rev.*, 2014, **43**, 205; (e) M. Liu, G. Ouyang, D. Niua and Y. Sang, *Org. Chem. Front.*, 2018, **5**, 2885; (f) T. S. Mahapatra, H. Singh, A. Maity, A. Dey, S. K. Pramanik, E. Suresh and A. Das, *J. Mater. Chem. C*, 2018, **6**, 9756; (g) A. Maity, A. Dey, M. K. Si, B. Ganguly and A. Das, *Soft Matter*, 2018, **14**, 5821; (h) A. Maity, F. Ali, H. Agarwalla, B. Anothumakkool and A. Das, *Chem. Commun.*, 2015, **51**, 2130; (i) A. K. Mandal, M. Gangopadhyay and A. Das, *Chem. Soc. Rev.*, 2015, **44**, 663; (j) A. Maity, M. Gangopadhyay, A. Basu, S. Aute, S. S. Babu and A. Das, *J. Am. Chem. Soc.*, 2016, **138**, 11113.
- (a) C. D. Jones and J. W. Steed, *Chem. Soc. Rev.*, 2016, **45**, 6546; (b) M. D. S. Maset, V. J. Nebot, J. F. Miravet and B. Escuder, *Chem. Rev.*, 2013, **42**, 7086; (c) N. M. Sangeetha and U. Maitra, *Chem. Soc. Rev.*, 2005, **34**, 821; (d) S. Datta and S. Bhattacharya, *Chem. Soc. Rev.*, 2015, **44**, 5596; (e) S.-M. Lu, J.-C. Huang, G.-T. Liu, Z.-W. Lin, Y.-T. Li, X.-H. Huang, C.-C. Huang and S.-T. Wu, *RSC Adv.*, 2017, **7**, 30979.
- (a) A. Panja and K. Ghosh, *Supramol. Chem.*, 2018, **30**, 722; (b) K. Ghosh, S. Panja and S. Bhattacharya, *ChemistrySelect*, 2017, **2**, 959; (c) A. Panja and K. Ghosh, *New J. Chem.*, 2018, **42**, 13718.
- (a) A. Caballero, R. Martinez, V. Lloveras, I. Ratera, J. V. Gancedo, K. Wurst, A. Tarraga, P. Molina and J. Veciana, *J. Am. Chem. Soc.*, 2005, **127**, 15666; (b) R. Martinez, A. Espinosa, A. Taraga and P. Molina, *Org. Lett.*, 2005, **7**, 5869; (c) M. Suresh, A. K. Mandal, S. Saha, E. Suresh, A. Mandoli, R. D. Liddo, P. P. Parnigotto and A. Das, *Org. Lett.*, 2010, **12**, 5406; (d) A. K. Saini, K. Natarajan and S. M. Mobin, *Chem. Commun.*, 2017, **53**, 9870; (e) A. Ghosh, S. Adhikari, S. Ta, A. Banik, T. K. Dangar, S. K. Mukhopadhyay, J. S. Matalobos, P. Brandão, V. Félix and D. Das, *Dalton Trans.*, 2016, **45**, 19491; (f) K. Tiwari, S. Kumar, V. Kumar, J. Kaur, S. Arora and R. K. Mahajan, *Spectrochim. Acta, Part A*, 2018, **191**, 16; (g) T. Wei, G. Liang, X. Chen, J. Qi, Q. Lin, Y. Zhang and H. Yao, *Tetrahedron*, 2017, **73**, 2938; (h) D. Ray, E. S. S. Iyer, K. K. Sadhu and P. K. Bharadwaj, *Dalton Trans.*, 2009, 5683.
- H. Svobodova, V. Noponen, E. Kolehmainen and E. Sievanen, *RSC Adv.*, 2012, **2**, 4985.
- (a) W. K. Jung, H. C. Koo, K. W. Kim, S. Shin, S. H. Kim and Y. H. Park, *Appl. Environ. Microbiol.*, 2008, **74**, 2171; (b) A. Y. Y. Tam and V. W. W. Yam, *Chem. Soc. Rev.*, 2013, **42**, 1540.
- H. T. Ratte, *Environ. Toxicol. Chem.*, 1999, **18**, 89.
- (a) T. A. Rouault, The role of iron regulatory proteins in mammalian iron homeostasis and disease, *Nat. Chem. Biol.*, 2006, **2**, 406; (b) E. C. Theil and D. J. Goss, *Chem. Rev.*, 2009, **109**, 4568.
- (a) J. F. Zhang, Y. Zhou, J. Yoon and J. S. Kim, *Chem. Soc. Rev.*, 2011, **40**, 3416; (b) S. K. Sahoo, D. Sharma, R. K. Bera, G. Crisponi and J. F. Callan, *Chem. Soc. Rev.*, 2012, **41**, 7195; (c) Y. S. Kim, G. J. Park, J. J. Lee, S. Y. Lee, S. Y. Lee and C. Kim, *RSC Adv.*, 2015, **5**, 11229; (d) A. Mitra, B. Ramanujam and C. P. Rao, *Tetrahedron Lett.*, 2009, **50**, 776; (e) P. Kumar, V. Kumar and R. Gupta, *RSC Adv.*, 2015, **5**, 97874; (f) S. Sen, S. Sarkar, B. Chattopadhyay, A. Moirangthem, A. Basu, K. Dhara and P. Chattopadhyay, *Analyst*, 2012, **137**, 3335.
- (a) J.-L. Zhong, X.-J. Jia, H.-J. Liu, X.-Z. Luo, S.-G. Hong, N. Zhanga and J.-B. Huang, *Soft Matter*, 2016, **12**, 191; (b) J.-F. Chen, Q. Lin, H. Yao, Y.-M. Zhang and T.-B. Wei, *Mater. Chem. Front.*, 2018, **2**, 999.

- 12 A. Y.-Y. Tam and V. W.-W. Yam, *Chem. Soc. Rev.*, 2013, **42**, 1540.
- 13 (a) W. Lin, L. Yuan, J. Feng and X. Cao, *Eur. J. Org. Chem.*, 2008, 2689; (b) L. Wang, L. Yang and D. Cao, *Sens. Actuators, B*, 2014, **202**, 949.
- 14 (a) J. Bachl, J. Mayr, F. J. Sayago, C. Cativiela and D. D. Diaz, *Chem. Commun.*, 2015, **51**, 5294; (b) Rajkamal, N. P. Pathak, D. Chatterjee, A. Paul and S. Yadav, *RSC Adv.*, 2016, **6**, 92225; (c) R. Roy, T. K. Adalder and P. Dastidar, *Chem. – Asian J.*, 2018, **13**, 552.
- 15 P. T. Chou, G. R. Wu, C. Y. Wei, C. C. Cheng, C. P. Chang and F. T. Hung, *J. Phys. Chem. B*, 2000, **104**, 7818.
- 16 A. R. Sarkar, C. H. Heo, M. Y. Park, H. W. Lee and H. M. Kim, *Chem. Commun.*, 2014, **50**, 1309.
- 17 (a) B. Adhikari, G. Palui and A. Banerjee, *Soft Matter*, 2009, **5**, 3452; (b) P. Chakraborty, B. Roy, P. Bairi and A. K. Nandi, *J. Mater. Chem.*, 2012, **22**, 20291.
- 18 (a) B. O. Okesola and David K. Smith, *Chem. Soc. Rev.*, 2016, **45**, 4226; (b) S. Samai and K. Biradha, *Chem. Mater.*, 2012, **24**, 1165; (c) P. C. Thomas, B. H. Cipriano and S. R. Raghavan, *Soft Matter*, 2011, **7**, 8192.
- 19 N. Venkatramaiah, S. Kumar and S. Patil, *Chem. Commun.*, 2012, **48**, 5007.
- 20 (a) D. Ownby, J. Belden, G. Lotufo and M. Lydy, *Chemosphere*, 2005, **58**, 1153; (b) P. Robidoux, J. Hawari and S. Thiboutot, *Environ. Toxicol. Chem.*, 1999, **23**, 1026; (c) A. H. Harris, O. F. Binkley and B. M. Chenoweth, *Am. J. Public Health*, 1946, **36**, 727.
- 21 (a) X. Cao, N. Zhao, H. Lv, Q. Ding, A. Gao, Q. Jing and T. Yi, *Langmuir*, 2017, **33**, 7788; (b) V. Bhalla, H. Singh, M. Kumar and S. K. Prasad, *Langmuir*, 2011, **27**, 15275; (c) V. Bhalla, A. Gupta, M. Kumar, D. S. S. Rao and S. K. Prasad, *ACS Appl. Mater. Interfaces*, 2013, **5**, 672; (d) Z. Hu, B. J. Deibert and J. Li, *Chem. Soc. Rev.*, 2014, **43**, 5815.